

The effect of BaTiO₃ particle shape on complex permittivity of 0.98MgTiO₃ – 0.02BaTiO₃ composite powders at GHz frequencies

M. Tuhkala^{1, a)}, M. Maček², T. Siponkoski¹, J. Juuti¹, M. Teirikangas¹, D. Suvorov² and H. Jantunen¹

¹ Microelectronics and Materials Physics Laboratories, University of Oulu, P.O. Box 4500, FIN-90014 Oulu, Finland

² Advanced Materials Department, Jožef Stefan Institute, Jamova cesta 36, SI-1000 Ljubljana, Slovenia

The effect of BaTiO₃ particle shape on the properties of 0.98MgTiO₃ – 0.02BaTiO₃ composite powders was characterized and analyzed using an indirectly coupled open-ended coaxial cavity resonator at gigahertz frequencies. Elongated micrometre sized BaTiO₃ particles were found to have a significantly stronger effect on permittivity when compared to composite powders having micro and nano sized spherical BaTiO₃ particles. Inclusion permittivities and dielectric loss tangents of composite powders increased from that of pure MgTiO₃ powder, 13.3 and 4.6×10^{-3} , up to 15.7 and 1.7×10^{-2} with needle shaped BaTiO₃ particles, respectively. The presented results give valuable information for tailoring the properties of dielectrics which can be utilized in the vast field of electronic component manufacturing.

KEYWORDS: A. ceramics, A. composites, A. electronic materials, D. dielectric properties, D. dielectrics

1. INTRODUCTION

Dielectric powdery substances are used in the extensive field of RF and electronics applications, for example, in polymer-ceramic composites and inks for printed electronics applications. These composites may consist of several different powdery parts as well as coatings which together determine both the mechanical and the electrical properties of the final product. Thus, by utilizing different dielectric materials, final products can be tailored to achieve desired properties, such as mechanical flexibility or dielectric losses, permittivity and capacitance in a certain frequency range. In particular, in specific narrowband filter applications a strict permittivity value is required without a compromise in frequency response as a function of operation temperature [1-4]. Therefore, the temperature coefficient can also be one of the limiting factors in the choice of volume ratio of the powdery materials [5-7]. In addition to the dielectric properties and molecular ratios of the materials used, the effective permittivity of composites can also be affected by different particle shapes and sizes. Using, for example, spherical, ellipsoidal, flake or needle shaped nano- and micrometre sized particles, the effect of a surrounding electric field varies, thus changing the total permittivity of the component [8-11]. Yet, the properties of powders and the influence of their particle shape in practice are poorly known, especially at high frequencies.

^{a)} Corresponding author. Electronic mail: mtuhkala@ee.oulu.fi

In this paper, the effect of BaTiO₃ particle shape on dielectric properties of 0.98MgTiO₃-0.02BaTiO₃ composite powders was characterized for the first time in powdery format using an indirectly coupled coaxial cavity resonator.

2. EXPERIMENTAL

Dielectric characterization of pure MgTiO₃ and 0.98MgTiO₃-0.02BaTiO₃ composite powders was done by using an open-ended coaxial resonator. A comprehensive and detailed description about the characterization method has been presented in journal paper previously reported by Tuhkala *et al.* [12]. The method was proved to be accurate for the characterization of magnesium and calcium titanate composite powders with varying molar ratios [13]. In the present experiment different sizes and shapes of BaTiO₃ particles were dosed into MgTiO₃, which is commonly used as the dielectric powder in composite applications, to form 0.98MgTiO₃-0.02BaTiO₃ composite powders [14]. The MgTiO₃ was a commercial dielectric powder from Alfa Aesar (99 %, +325 mesh, formula weight 120.21 g/mol). Needle shaped micrometre size BaTiO₃ particles (formula weight 233.2 g/mol, density 5.47 g/cm³) were prepared in the Jožef Stefan Institute, Slovenia. These particles were formed under hydrothermal conditions at + 240 °C from sodium titanate belts in an alkaline (CNaOH = 0.07 mol/l) water solution of barium acetate. These elongated BaTiO₃ particles had average thickness and length of 270 nm and 2 µm, respectively (Fig. 1).

Spherical shaped BaTiO₃ particles were supplied by Alfa Aesar (99.7 %, Metal basis, formula weight 233.19 g/mol, density 5.85 g/cm³) and Sachtleben (P23757, formula weight 233 g/mol, density 5.78 g/cm³). The crystal structures of the powder particles were determined using X-ray diffraction and pattern matching (Discover D8, Bruker AXS) between 2θ angles of 20-70°. In the case of BaTiO₃ powders, crystal phases were also investigated using TOPAS 4.2. software (Bruker AXS) and Rietveld refinement. In the refinement powders were assumed to have tetragonal and also a very small amount of cubic phases. For the tetragonal structure the Z-coordinate of Ti and O atoms were refined, thus allowing for distortion of the tetragonal structure and enabling better fitting. Particle densities of MgTiO₃ and BaTiO₃ powder particles were measured using Archimedes' method, a pycnometer (Gay-Lussac BlauBrand[®], Brand GmbH + Co KG, Germany) and clean de-ionized water. Densities of composite powder particles were calculated using the densities and molar ratios of magnesium and barium titanate powders. Specific surface areas (SSA) were analyzed using the BET-method based on nitrogen gas adsorption on particles at the temperature of liquid nitrogen (ASAP[™] 2020, Micromeritics Instrument Corporation, U.S.A.). Nanoparticle sizes were analyzed using a laser diffraction based method (Beckman Coulter LS 13 320). It should be noted that agglomerates, especially with non-coated nanometre sized particles, may affect the determined particle sizes. Master samples (5 g) were prepared using a precision balance (Precisa XB 620 M) and thorough dry mixing in geometric series in order to obtain well-homogenized powder composite mixtures. The master samples were preserved for one week in a silica filled desiccator to avoid moisture adsorption. The dielectric characterization was done at room temperature (+21 °C) and a relative humidity of 16%.

The characterization of pure MgTiO₃ and 0.98MgTiO₃-0.02BaTiO₃ composite powders were done using six different volume fractions between 10-50% of theoretical density which filled the sample cavity (1.092 cm³). In order to get homogenous filling of the cavity vibration and compression were used during the filling process. Frequency responses, i.e., resonance frequency (f_r) and quality factor (Q), of an empty ($f_r = 4.55$ GHz, Q = 1200) and sample filled resonator were measured using a vector network analyzer (Rohde and Schwartz ZVB 20 GHz) and -35 dB coupling strength.

Inclusion permittivities of MgTiO_3 and $0.98\text{MgTiO}_3\text{-}0.02\text{BaTiO}_3$ composite powders were determined using the measurement results of effective permittivities and the mixing equations of Bruggeman symmetric (Eq. 1) and Looyenga (Eq. 2). These equations had previously been found to have good correlation in the characterization of dielectric properties of particles reported by Tuhkala *et al.*, Conger *et al.* and Nelson *et al.* [12, 13, 15-18].

$$\frac{\varepsilon_i - \varepsilon_{eff}}{\varepsilon_i + 2\varepsilon_{eff}} f + \frac{\varepsilon_e - \varepsilon_{eff}}{\varepsilon_e + 2\varepsilon_{eff}} (1 - f) = 0 \quad (1)$$

$$\varepsilon_{eff}^{1/3} = (1 - f)\varepsilon_e^{1/3} + f\varepsilon_i^{1/3}, \quad (2)$$

where ε_{eff} , ε_e , ε_i are the effective permittivity of the medium, permittivities of the matrix (e.g., air, $\varepsilon_r = 1.00059$) and inclusion respectively, and f is the volume fraction of the inclusions. Inclusion permittivities were determined at volume fraction 0.43 where the mixing equations define the same theoretical effective permittivity. In addition, a certain compaction level ($f > 0.25$) was required in order to get comparable results as reported by Sheen *et al.* and Macutkevic *et al.* [19, 20]. The determined inclusion permittivity was a combination of permittivities of the MgTiO_3 and BaTiO_3 particles.

The effective loss tangents ($\tan \delta_{eff}$) of powders were calculated using the differences in quality factors of an empty and sample filled resonator (Eq. 3).

$$\tan \delta_{eff} = \frac{1}{Q_{filled}} - \frac{1}{Q_{empty}} \quad (3)$$

By using a general mixing model in parallel mode (Eq. 4) and the volume fraction of the dielectric material (f_d) the dielectric loss tangent ($\tan \delta_d$) was derived (Eq. 5). It should be noted that the dielectric loss tangent of the air is close to zero [21].

$$(\tan \delta_{eff})^\alpha = \sum f_i (\tan \delta_i)^\alpha \quad (4)$$

$$\tan \delta_d = \frac{\tan \delta_{eff}}{f_d} \quad (5)$$

In the general mixing model (Eq. 4) the power α determines the mixing model, i.e., $-1 = \text{serial}$, $0 = \text{logarithmic}$ and $1 = \text{parallel}$ and the subscript i refers to the volume fraction and dielectric loss tangent of the i^{th} material. The parallel mode was shown to have good correlation in the determination of dielectric loss and molar ratios of composite powders reported by Tuhkala *et al.*, Huang *et al.* and Fukuda *et al.* [13, 15, 22, 23].

3. RESULTS AND DISCUSSION

The addition of different sizes and shapes of BaTiO_3 particles resulted in significantly changed dielectric properties when compared to pure MgTiO_3 powder (Fig. 2). The increase in effective permittivity was found to be systematic and significant, even with the lowest volume fractions. The highest increase in effective permittivity was observed for the needle shaped BaTiO_3 particles

obtaining an inclusion permittivity of 15.7 for 0.98MgTiO₃-0.02BaTiO₃ composite powder. The spherical shaped nanometre sized BaTiO₃ particles caused nearly as great an increase in permittivity with the lowest volume fraction ($f = 0.16$). However, effective permittivities with denser samples were lower than those with the needle shaped particles and thus an inclusion permittivity of 14.2 was determined at volume fraction $f \approx 0.43$ used for comparison. The needle shaped micrometre sized BaTiO₃ particles were found to increase effective permittivities of the composite powder rapidly above a volume fraction 0.19 compared to nanometre sized spherical particles. This correlates also with the electrostatic theory [24] and mathematical analysis regarding needle shaped particles reported by Jones *et al.* [9]. With micrometre sized spherical BaTiO₃ particles the effective permittivities of the composite powder were not increased as rapidly as a function of loading, which resulted in a determined inclusion permittivity of 13.7.

As was found with the permittivity, the needle shaped particles also efficiently increased the effective loss tangents resulting in a dielectric loss tangent of 1.7×10^{-2} for 0.98MgTiO₃-0.02BaTiO₃ inclusions. The spherical shaped BaTiO₃ particles increased the dielectric loss tangent from that of pure MgTiO₃, i.e., from 4.6×10^{-3} , to 5.4×10^{-3} and 9.7×10^{-3} with micro- and nanometre sized BaTiO₃ particles, respectively. All measurement results are summarized in Table 1.

From the results it can be clearly seen that a higher permittivity was reached with needle shaped particles when compared to spherical particles. Because of differences in BaTiO₃ particle shapes, percolation and thus also interactions between particles were different and this can affect the permittivity of the composite powder [25]. Correlation with this was found with the measurement results of effective permittivities and loss tangents that increased systematically with all measured powder samples as shown in Fig. 2.

The XRD measurements and Rietveld refinement (inserts) of the BaTiO₃ powders are presented in Fig. 3. The P4mm tetragonal and Pm-3m cubic models were selected for the data fitting according to the results from the pattern matching. The relative amount of tetragonal phase was more than 95 % in all of the powders. The highest tetragonality, i.e., the ratio between lattice parameters c and a , of ~ 1.009 was observed with the 1.17 μm spherical BaTiO₃ particles. The tetragonality of both the 0.15 μm spherical and needle shaped particles was ~ 1.006 . This was also seen as a change in the separation of 002 and 200 peaks in Fig. 3. The 0.15 μm spherical particles were found to be slightly less tetragonal than the 1.17 μm spherical particles. However, even with such small molar amounts of BaTiO₃ particles they still provided a greater change in permittivity (Fig. 4). A similar effect was reported by Dhir *et al.* [26] and Zou *et al.* [27] in their researches of nanosize-scale Dy-doped BiFeO₃, and the effect of particle size on the BaTiO₃ ceramics, respectively. In addition, M. Teirikangas *et al.* reported that changes in interfaces, due to higher specific surface area, between polymer matrix and nanoparticles were the reason for the increased permittivity [28].

Particles with higher SSA can increase moisture adsorption and the scattering of an incident electromagnetic wave at high frequencies which can increase losses [29]. However, geometrically different form factor can affect magnitude of scattering and thus cause changes in total loss mechanism of the wave [29]. Furthermore, it should be noted that agglomerates of nanoparticles may affect the total permittivity differently compared to optimally distributed composite powders due to interactions between particles [30]. Although the used theoretical models of Bruggeman symmetric and Looyenga are tailored for spherical shaped particles they correlated well with the composite powder containing needle shaped BaTiO₃ particles (Fig. 4). This is due to the fact that the needle shaped particles represent only a small fraction of the material. In the case where they

would be the primary filler, some other equation should be used to take into account the aspect ratio of the particles.

4. CONCLUSIONS

Even though the powder components in the presented examples of composite powders were similar regarding their chemical composition, relevant changes in the dielectric properties of 0.98MgTiO₃-0.02BaTiO₃ composite powders were achieved by varying the sizes and shapes of the BaTiO₃ particles. The composite powders had remarkable differences in their effective permittivities and loss tangents. The needle shaped micrometre sized BaTiO₃ particles had the greatest effect on the effective permittivity amongst all the measured samples, thus resulting in an inclusion permittivity of 15.7 and a dielectric loss tangent of 1.7×10^{-2} . In addition to the finding that needle shaped particles can affect the permittivity of the composite significantly more than spherical nanoparticles powders, even with low molar ratios, it also highlights the importance of measuring dielectric properties of powdery substances. As demonstrated in the present paper, properties of the final product could be tailored simply by varying the particle shapes of dielectric powdery materials. This information could be utilized, for example, in a production of electrical composites for RF applications.

ACKNOWLEDGEMENT

The authors gratefully acknowledge the project “Innoinks” 906/31/2010 funded by Tekes (FIN), Sachtleben Pigments Oy (FIN), Pulse Finland Oy (FIN) and NOF Corporation (JAP). The work has received funding from the European Research Council (ERC) grant agreement No. 291132. Author Jari Juuti acknowledges the funding of the Academy of Finland (project numbers 273663 and 267573).

REFERENCES

- [1] M. Kadota, T. Nakao, T. Murata and K. Matsuda, "Surface acoustic wave filter in high frequency range with narrow bandwidth and excellent temperature property," in *IEEE International Ultrasonics Symposium Proceedings*, Beijing, 2008.
- [2] C.-H. Shen and C.-L. Huang, "Microwave dielectric properties of (Mg_{0.95}Ni_{0.05}) TiO₃-SrTiO₃ ceramics with a near-zero temperature coefficient of resonant frequency," *International Journal of Applied Ceramic Technology*, vol. 7, no. 2, pp. 207 - 216, 2010.
- [3] A. Yokoi, H. Ogawa and A. Kan, "Microwave dielectric properties of BaO-Ta₂O₅-TiO₂ system," *Journal of the European Ceramic Society*, vol. 26, no. 10-11, pp. 2069 - 2074, 2006.
- [4] C.-L. Huang, C.-L. Pan and J.-F. Hsu, "Dielectric properties of (1-x)(Mg_{0.95}Co_{0.05})TiO₃-xCaTiO₃ ceramic system at microwave frequency," *Materials Research Bulletin*, vol. 37, no. 15, p. 2483-2490, 2002.
- [5] L. Li, X. M. Chen and C. X. Fan, "Microwave dielectric characteristics and finite element analysis of MgTiO₃-CaTiO₃ layered dielectric resonators," *Journal of the European Ceramic Society*, vol. 26, no. 15, pp. 3265-3271, 2006.
- [6] P. Fiorenza, R. Lo Nigro, P. Delugas, V. Raineri, A. G. Mould and D. C. Sinclair, "Direct imaging of the core-shell effect in positive temperature coefficient of resistance-BaTiO₃ ceramics," *Applied Physics Letters*, vol. 95, no. 14, pp. 142904-1 -142904-3, 2009.
- [7] E. S. Choi, . Y. H. Lee and S. G. Bae, "Microwave dielectric properties of MgTiO₃-BaTiO₃ ceramics," *Proceedings of the International Symposium on Electrical Insulating Materials*, pp. 99-102, 2001.
- [8] R.-B. Yang, W.-F. Liang, S.-T. Choi and C.-K. Lin, "The effects of size and shape of iron particles on the microwave absorbing properties of composite absorbers," *IEEE Transactions on Magnetics*, vol. 49, no. 7, pp. 4180 - 4183, 2013.
- [9] S. B. Jones and S. P. Friedman , "Particle shape effects on the effective permittivity of anisotropic or isotropic media consisting of aligned or randomly oriented ellipsoidal particles," *Water Resources Research*, vol. 36, no. 10, pp. 2821 - 2833, 2000.
- [10] H. S. Göktürk, T. J. Fiske and D. M. Kalyon, "Effects of particle shape and size distributions on the electrical and magnetic properties of nickel/polyethylene composites," *Journal of Applied Polymer Science*, vol. 50, no. 11, pp. 1891 - 1901, 1993.

- [11] Z.-M. Dang, Y. Zheng and H.-P. Xu, "Effect of the ceramic particle size on the microstructure and dielectric properties of barium titanate/polystyrene composites," *Journal of Applied Polymer Science*, vol. 110, no. 6, pp. 3473 - 3479, 2008.
- [12] M. Tuhkala, J. Juuti and H. Jantunen, "Method to characterize dielectric properties of powdery substances," *Journal of Applied Physics*, vol. 114, no. 1, 2013.
- [13] M. Tuhkala, J. Juuti and H. Jantunen, "An indirectly coupled open-ended resonator applied to characterize dielectric properties of MgTiO₃-CaTiO₃ powders," *Journal of Applied Physics*, vol. 115, no. 18, pp. 184101 - 184101-5, 2014.
- [14] M. T. Sebastian, "alumina, titania, ceria, tungstate and other materials," in *Dielectric materials for wireless communication*, Amsterdam, Elsevier Science Publishers, 2008, pp. 425 - 426, 429 - 430, 516 - 517.
- [15] M. Tuhkala, J. Juuti and H. Jantunen, "Use of an open-ended coaxial cavity method to characterize powdery substances exposed to humidity," *Applied Physics Letters*, vol. 103, no. 14, pp. 142907-1-142907-4, 2013.
- [16] M. Tuhkala, J. Juuti and H. Jantunen, "Determination of complex permittivity of surfactant treated powdery substances by an open-ended coaxial cavity resonator," *Journal of Applied Physics*.
- [17] N. L. Conger and S. E. Tung, "Measurement of Dielectric Constant and Loss Factor of Powder Materials in the Microwave Region," *The Review of Scientific Instruments*, vol. 38, no. 3, pp. 384-386, 1967.
- [18] S. O. Nelson and P. G. Bartley, "Open-Ended Coaxial-Line Permittivity Measurements on Pulverized Materials," *IEEE TRANSACTIONS ON INSTRUMENTATION AND MEASUREMENT*, vol. 47, no. 1, pp. 133-137, 1998.
- [19] J. Macutkevic and J. Banys, "Comment on "giant dielectric permittivity of detonation-produced nanodiamond is caused by water" by S. S. Batsanov, S. M. Gavrilkin, A. S. Batsanov, K. B. Poyarkov, I. I. Kulakova, D. W. Johnson and B. G. Mendis, J. Mater. Chem., 2012, 22, 11166," *Journal of Materials Chemistry C*, vol. 1, no. 19, pp. 3255 -3256, 2013.
- [20] J. Sheen and Z. W. Hong, "Microwave measurements of dielectric constants by exponential and logarithmic mixture equations," *Progress In Electromagnetics Research*, vol. 100, pp. 13-26, 2010.

- [21] X. Jin and M. Ali, "Embedded antennas in dry and saturated concrete for applications in wireless sensors," *Progress In Electromagnetics Research*, vol. 102, pp. 197-211, 2010.
- [22] C.-L. Huang and M.-H. Weng, "Improved high q value of $\text{MgTiO}_3\text{-CaTiO}_3$ microwave dielectric ceramics at low sintering temperature," *Materials Research Bulletin*, vol. 36, no. 15, p. 2741–2750, 2001.
- [23] K. Fukuda, R. Kitoh and I. Awai, "Microwave characteristics of $\text{TiO}_2\text{-Bi}_2\text{O}_3$ dielectric resonator," *Japanese Journal of Applied Physics*, vol. 32, no. 10, pp. 4584-4588, 1993.
- [24] A. Sihvola, "Advanced mixing principles," in *Electromagnetic mixing formulas and applications*, London, United Kingdom, The Institution of Electrical Engineers, 1999, pp. 61-71.
- [25] A. Sihvola, "Special phenomena caused by mixing," in *Electromagnetic Mixing Formulas and Applications*, London, United Kingdom, The Institution of Electrical Engineers, 1999, pp. 215 - 233.
- [26] G. Dhir, P. Uniyal and N. K. Verma, "Effect of Particle Size on Magnetic and Dielectric Properties of Nanoscale Dy-Doped BiFeO_3 ," *Journal of Superconductivity and Novel Magnetism*, vol. 27, no. 6, pp. 1569 - 1577, 2014.
- [27] Y. Zou, Y. Wu, X. Guo, S. Tong, Z. Wang and L. Zhang, "Effect of particle size on the densification and dielectric properties of BaTiO_3 ceramics prepared by liquid phase sintering," *Physica Status Solidi. A*, vol. 209, no. 2, pp. 243 - 247, 2012.
- [28] M. Teirikangas, J. Juuti and H. Jantunen, "Organic-inorganic RF composites with enhanced permittivity by nanoparticle additions," *Progress In Electromagnetic Research*, vol. 115, pp. 147 - 157, 2011.
- [29] A. Sihvola, "Towards higher frequencies," in *Electromagnetic mixing formulas and applications*, London, United Kingdom, The Institution of Electrical Engineers, 1999, pp. 177 - 193.
- [30] A. Sihvola, "Classical mixing approach," in *Electromagnetic mixing formulas and applications*, London, United Kingdom, The institution of Electrical Engineers, 1999, pp. 39-47.
- [31] Alfa Aesar, "Alfa Aesar, Certificate of analysis MgTiO_3 , LOT J22W049," 9 February 2015. [Online]. Available: <http://www.alfa.com>. [Accessed 9 February 2015].

[32] Alfa Aesar, "Alfa Aesar, Certificate of analysis BaTiO₃, LOT 61400271," 9 February 2015. [Online]. Available: <http://www.alfa.com>. [Accessed 9 February 2015].

TABLES

Table 1. Particle shapes, sizes and SSA-values of MgTiO₃ and BaTiO₃ particles. Densities and dielectric properties of MgTiO₃ and 0.98MgTiO₃-0.02BaTiO₃ composite powder inclusions.

Powder	Particle shape	Particle size ^a [μm]	SSA [m ² / g]	ρ [g / cm ³]	ε _i	tan δ _d [× 10 ⁻³]	Phase
MgTiO ₃	Spherical	3.06 [31]	3.5	3.95	13.3	4.6	-
0.98MgTiO ₃ - 0.02BaTiO ₃	Needle ^b	2 (0.27) ^b	5.3 ^b	4.0	15.7	17	Tetragonal ^b
0.98MgTiO ₃ - 0.02BaTiO ₃	Spherical ^b	0.15 ^b	6.0 ^b	4.0	14.2	9.7	Tetragonal ^b
0.98MgTiO ₃ - 0.02BaTiO ₃	Spherical ^b	1.17 ^b [32]	2.0 ^b [32]	4.0	13.7	5.4	Tetragonal ^b

^a Particle size (d₅₀) where 50% of particles represent the size.

^b Properties of BaTiO₃ particles. Thickness of the needle shaped BaTiO₃ particles in brackets.

TABLE OF FIGURES

Fig. 1. SEM figure of elongated BaTiO₃ particles.

Fig. 2. Effective permittivity and loss tangent values of composite and MgTiO₃ powders as a function of volume fraction. Determined dielectric values of inclusions are presented as inserts. Sizes and shapes of BaTiO₃ particles are in brackets. Resonance frequencies of the measurements were within the range of 2.2 – 3.7 GHz.

Fig. 3. X-ray diffraction of the used BaTiO₃ powders between 2θ angles of 20-70° with orientations. Diffraction between 2θ angles of 44.5 – 46, as insert (a = spherical 0.15 μm , b = spherical 1.17 μm and c = needle 2 μm), indicated tetragonal phase.

Fig. 4. Theoretical curves of Bruggeman symmetric and Looyenga mixing models, measured effective permittivities and loss tangents of powder composites as a function of volume fraction. Sizes and shapes of BaTiO₃ particles are in brackets. Resonance frequencies of the measurements were within the range of 2.2 – 3.7 GHz.

FIGURES

Fig. 1.

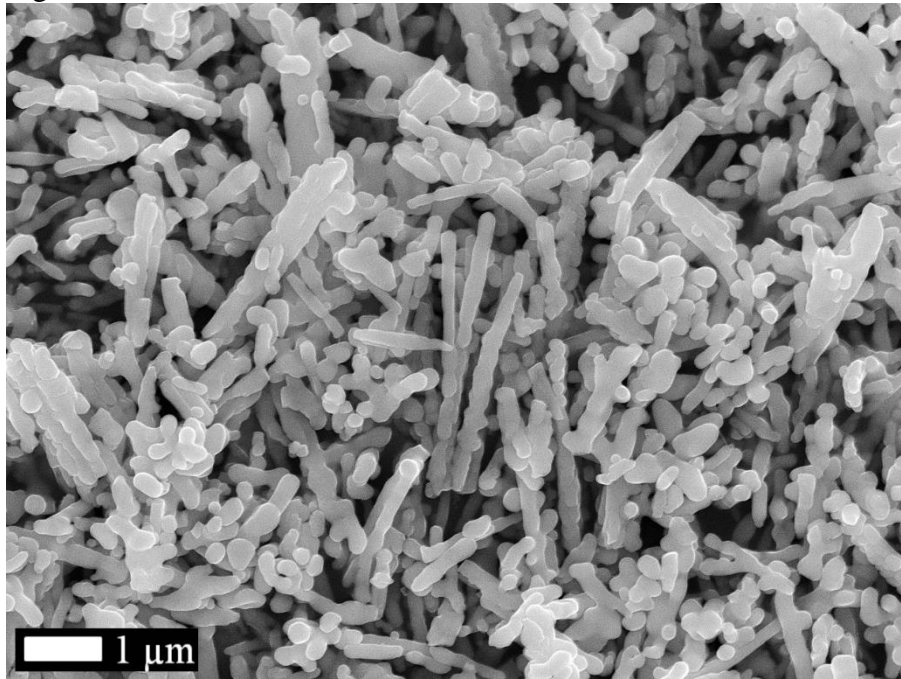


Fig. 2.

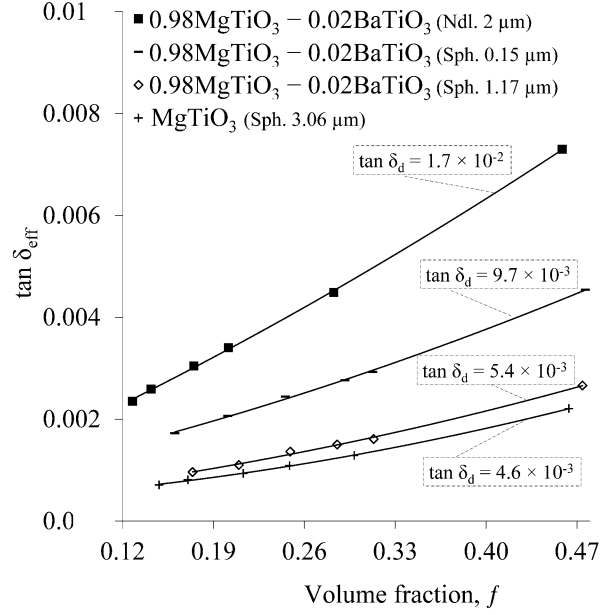
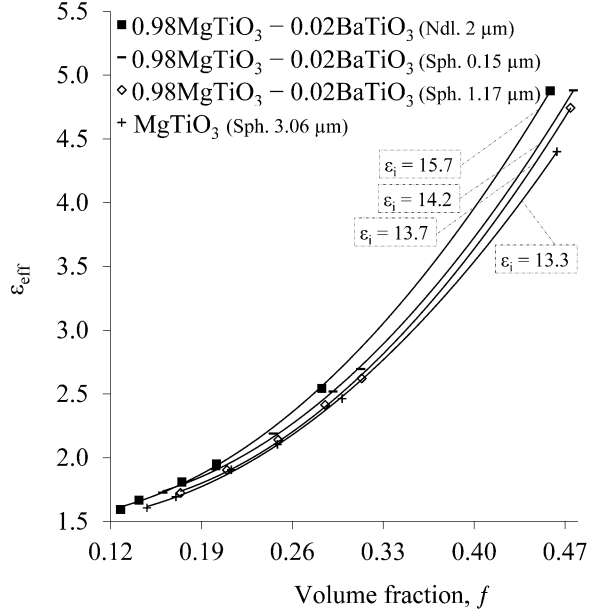


Fig. 3.

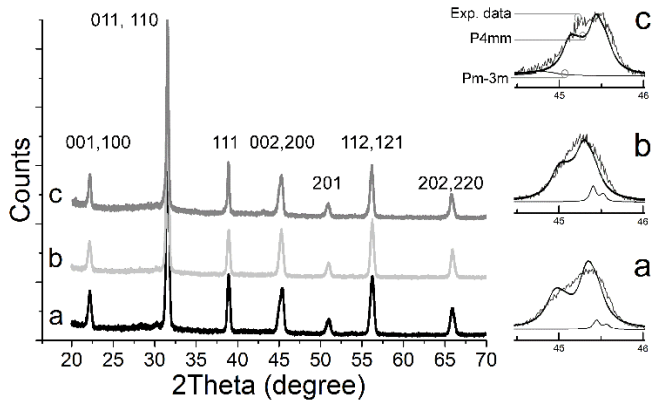


Fig. 4.

